Maurocalcine interacts with the cardiac ryanodine receptor without inducing channel modification.

Xavier Altafaj, Julien France, János Almássy, Istvan Jona, Daniela Rossi, Vincenzo Sorrentino, Kamel Mabrouk, Michel de Waard, Michel Ronjat

Maurocalcine interacts with cardiac ryanodine receptor without inducing channel modification.

Xavier Altafaj[‡], Julien France[‡], Janos Almassi[¶], Istvan Jona[¶], Daniela Rossi[§], Vincenzo Sorrentino[§]. Kamel Mabrouk[¦] , Michel De Waard[‡] and Michel Ronjat[‡*].

‡iRTSV/CCFP CEA Grenoble INSERM U836 (équipe 3) Institut des Neurosciences Grenoble GIN, 17 rue des Martyrs, 38054 Grenoble Cedex 09, France.

¶Department of Physiology, Research Center of Molecular Medicine, Medical and Health Science Center, University of Debrecen Hungary.

§Molecular Medicine Section, Department of Neuroscience, University of Siena, Siena, Italy

¦ CNRS FRE 2738, Laboratoire Ingénierie des Protéines, IFR Jean Roche, Boulevard Pierre Dramard, 13916 Marseille Cedex 20, France

- Address correspondence to : Dr Michel Ronjat, iRTSV/CCFP CEA Grenoble INSERM U836 (équipe 3) Institut des Neurosciences Grenoble GIN, 17 rue des Martyrs, 38054 Grenoble Cedex 09, France.. Tel: 33 4 38 78 46 69 ; Fax: 33 4 38 78 50 41 ; E-Mail: mronjat@cea.fr

Synopsis

We have previously shown that maurocalcine (MCa), a toxin from the venom of the scorpion *Maurus palmatus*, binds to type 1 ryanodine receptor (RyR1) and induces strong modifications of its gating behaviour. In this study, we investigated the ability of MCa to bind on and modify the gating process of cardiac, type 2, ryanodine receptor (RyR2). By performing pull-down experiments we show that MCa directly interacts with RyR2 with an apparent affinity of 150 nM. By expressing *in vitro* different domains of RyR2, we show that MCa binds on two domains of RyR2 homologous to those previously identified on RyR1. The effect of MCa binding on RyR2 was then evaluated by three different approaches: i) [^{3}H]-ryanodine binding experiments, showing a very weak effect of MCa (up to 1 µM), ii) calcium release measurements from cardiac sarcoplasmic reticulum vesicles, showing that MCa up to 1 µM is unable to induce Ca^{2+} release and, iii) single channel recordings, showing that MCa has no effect on the open probability or on RyR2 channel conductance level. Long lasting opening events of RyR2 were observed in the presence of MCa only when the ionic current direction was opposite to the physiological direction, i.e. from the cytoplasmic face of RyR2 to its luminal face. Therefore, despite the conserved MCa binding ability of RyR1 and RyR2, functional studies show that, in contrast to what observed with RyR1, MCa does not affect the gating properties of RyR2. These results highlight a different role of the MCa binding domains in the gating process of RyR1 and RyR2.

Introduction

Calcium signaling is a crucial step in the regulation of major cellular functions. Oscillations of cytosolic Ca^{2+} concentration result from the balance between mechanisms allowing cytoplasmic Ca^{2+} increase (influx from extracellular medium and release from intracellular stores) and their counterparts allowing Ca^{2+} storage in endoplasmic reticulum (ER) and Ca^{2+} efflux. Calcium release from ER is due to the activation of two different families of intracellular Ca^{2+} channels, the ryanodine receptors (RyRs) and the IP3 receptors (IP3Rs). RyRs family is composed of three protein isoforms encoded by three different genes: RyR1 or "skeletal muscle" isoform, RyR2 or "cardiac muscle" isoform and RyR3 isoform showing a ubiquitous expression pattern [1]. Although the three isoforms exhibit a relatively conserved amino acid sequence and an overall similar regulation by cytoplasmic Ca^{2+} concentration and various effectors, different mechanisms have been proposed to control their activation following plasma membrane depolarization. Indeed, while physiological RyR2 activation requires the Ca^{2+} influx through the cardiac dihydropyridine receptor (DHPR), according to the mechanism of "calcium-induced calcium release" (CICR), RyR1 has been proposed to be "conformationally" coupled to the DHPR skeletal isoform and to be activated in answer to charges movement within the DHPR following plasma membrane depolarization. The molecular bases of these processes have been investigated by studying the coupling between DHPR and RyR when expressing different pairs of isoforms. Expression of a cardiac DHPR $Ca_v1.2$ subunit in skeletal muscle cells of dysgenic mice ($Ca_v1.1^{-/-}$) as well as expression of RyR2 in skeletal muscle cells lacking RyR1 results in CICR process [2, 3]. These results clearly indicate that the differences in RyR physiological regulation process rely not only on the DHPR moiety but also on intrinsic gating properties specific of each RyR isoform.

Toxins issued from spiders, snakes or scorpions venoms are strong effectors of ion channels, converting these peptides in very valuable tools for the study of channel properties. In the last decade four scorpion toxins, Imperatoxin A (IpTxA), Maurocalcine (MCa) and *Buthodus judaicus* toxins 1 and 2 (BjTx-1,2) have been shown, *in vitro*, to activate RyR1 [4-6]. Although all of them promote an increase of [^{3}H]-ryanodine binding on RyR1 and induce RyR1 opening at subconductance states, MCa appears as the strongest effectors of RyR1 in

terms of affinity, increase of ryanodine binding and duration of the induced subconductance opening events.

Using site directed mutagenesis approach, we identified a stretch of basic amino acid residues critical for MCa effect on RyR1 [7]. Interestingly this domain shows some sequence similarities with a discrete region (domain A) of the cytoplasmic II-III loop of the DHPR $Ca_v1.1$ subunit, the physiological activator of RyR1 in skeletal muscle [8]. Based on this similarity, MCa and IpTxA have been used to study the functional role of the DHPR domain A [9, 10]. In skeletal muscle cells, these toxins have been shown to increase the frequency and to modify the characteristics of RyR1-mediated Ca^{2+} release events [11, 12].

We recently identified two discrete domains of RyR1 responsible for its interaction with MCa [13]. We showed that these two domains also bind a synthetic peptide corresponding to domain A of the DHPR. These results strengthened the hypothesis that MCa mimics the effect of domain A on RyR1. The fact that these amino acid sequences are relatively conserved between RyR1 and RyR2 prompted us to evaluate the binding and functional effect of MCa on RyR2.

In this work, we demonstrate that MCa physically interacts with the purified RyR2 isoform. This interaction takes place within amino acid regions of RyR2 homologous to the previously identified MCa binding domains of RyR1. However, in sharp contrast to what is observed on RyR1, we show that MCa has negligible effect on [^{3}H]-ryanodine binding on RyR2, fails to induce Ca^{2+} release from cardiac SR vesicles and does not modify gating properties of purified RyR2 incorporated into planar lipid bilayer. These results highlight a different involvement of the MCa binding domains in the control of the gating process of RyR1 and RyR2.

Experimental

Cloning and expression of RyR1 and RyR2 fragments – RyR1 and RyR2 cDNAs (GenBank™ accession numbers X15750 and M59743, respectively) coding for the fragments F3 (aa 1022-1631 and 1033-1622, respectively) and F7 (aa 3201-3661 and 3158-3609, respectively) were cloned by a PCR-based approach. RyR1 fragments were cloned in the pSG5 vector (Stratagene) and RyR2 fragments were cloned in pcDNA3.1/myc vector (Invitrogen).

RyR fragments were then expressed using a coupled *in vitro* transcription and translation system (TNT™ kit, Promega), allowing the obtention of [^{35}S]-labeled RyR1 or RyR2 F3 and F7 fragments.

Heavy sarcoplasmic reticulum (HSR) vesicles preparation

HSR vesicles from rabbit skeletal muscle were prepared as described in [14]. Cardiac HSR vesicles where prepared from canine heart left ventricle muscle as described in [15]. Protein concentration was measured by the Bradford method.

Ryanodine receptor purification.

RyR1 and RyR2 were purified from CHAPS-solubilized skeletal and cardiac muscle HSR vesicles by the sucrose gradient technique [15, 16].

Pull-down experiments - Polystyrene magnetic beads (500 µg) coated with streptavidine (Dynal) were incubated for 30 min at room temperature in phosphate saline buffer (PBS pH 7.4) in the presence of biotinylated MCa (40 µM final concentration) or biotin (control) and then washed three times with PBS. MCa (or biotin) coated beads where incubated with purified RyR1, purified RyR2 or [^{35}S]RyR2 fragments, for 2 hrs at room temperature in a buffer (buffer A) containing 150 mM NaCl, 20 mM HEPES, pH 7.4, 2 mM EGTA and 2 mM CaCl2 (pCa5) supplemented with proteases inhibitors and BSA 0.1 mg/ml. For the measure of the apparent MCa binding affinity on RyR2, streptavidine beads were coated with different amounts of biot-MCa (corresponding to the indicated concentrations) and then incubated with RyR2 in buffer A in the presence of 10 nM [^{3}H]-ryanodine. After washing three times with PBS, bound proteins were eluted and analyzed by Western blot (for RyR1 and RyR2 pull down experiments), autoradiography (for pull down of [^{35}S] labelled RyR fragments) after separation on SDS-PAGE or liquid scintillation counting (for pull down of [^{3}H] ryanodine labelled RyR2). RyRs where identified using polyclonal antibodies recognizing the different

RyR isoforms [14]. Each experiment was performed at least three times. Data are presented as mean ± S.E. M.

[^{3}H]-ryanodine binding assay - Heavy SR vesicles (cardiac or skeletal; 1 mg/ml) were incubated at 37°C for 2.5 hrs in buffer A in the presence of 5 nM [^{3}H]-ryanodine. MCa was added to the assay buffer just prior to the addition of HSR vesicles. After incubation, HSR vesicles were filtrated through Whatmann GF/B glass filters and washed three times with 5 ml of ice-cold washing buffer composed of 150 mM NaCl, 20 mM HEPES, pH 7.4. [^{3}H]-ryanodine bound to filters was then measured by liquid scintillation counting. Non-specific binding was measured in the presence of 20 µM unlabelled ryanodine. Each experiment was performed in triplicate and repeated at least twice. All of the data are presented as the mean ± S.E. M.

RyR2 Ca^{2+} channel reconstitution and single-channel recording analysis – Channel activity measurements were carried out using purified RyR2 incorporated into planar lipid bilayer. The bilayers were formed using phosphatidylethanolamine, phosphatidylserine, and L-phosphatidylcholine in a ratio of 5:4:1 dissolved in *n*-decane up to the final lipid concentration of 20 mg/ml. Bilayers were formed across a 200- or 250-µm diameter aperture of a Delrin cap using a symmetrical buffer solution (250 mM KCl, 100 µM EGTA, 150 µM $CaCl_2$, 20 mM PIPES, pH 7.2). A small aliquot of purified RyR2 was added into one chamber. After successful incorporation we tested the effect of calcium of both sides in order to determine the orientation of the incorporated channel. The cytoplasmic and luminal sides were defined as “cis” and “trans” side respectively. For the determination of the gating properties of the channel, the calcium concentration was adjusted to 472 nM on the cis side by addition of EGTA. Electrical signals were filtered at 1 kHz through an 8-pole low-pass Bessel filter and digitized at 3 kHz using Axopatch 200 and pCLAMP 6.03 (Axon Instruments, Union City, CA).

Ca^{2+} release measurements - Ca^{2+} release from skeletal or cardiac HSR vesicles was measured using the Ca^{2+}-sensitive dye antipyrylazo III. The absorbance was monitored at 710 nm by a diode array spectrophotometer (MOS-200 Optical System, Biologic, Claix, France). Vesicles (50 µg) were actively loaded with Ca^{2+} at 37 °C in 2 ml of a buffer containing 100 mM KCl, 7.5 mM sodium pyrophosphate, 20 mM MOPS, pH 7.0, supplemented with 250 µM antipyrylazo III and 1 mM ATP/$MgCl_2$. Ca^{2+} loading was initiated by sequential additions of 20 µM (final concentration) of $CaCl_2$. At the end of each experiment, Ca^{2+} remaining in the vesicles was determined by the addition of Ca^{2+} ionophore A23187 (4 µM) and the

absorbance signal calibrated by two consecutive additions of 20 µM $CaCl_2$. Total recording time in each experiment was 10–20 min for each experimental condition tested. In these conditions, no spontaneous calcium release was observed.

Results

MCa interacts with purified RyR2.

The interaction of MCa with RyR2, was investigated using a synthetic MCa with a biotinylated lysine at the amino terminus, immobilized on streptavidine-coated beads as previously described [13]. Using these MCa-covered beads, we performed pull-down experiments with purified RyR1 and RyR2 preparation. Figure 1A shows that both isoforms of RyR (RyR1 in lane 1 and RyR2 in lane 4) interact with the MCa-coated beads (lanes 3 and 6), while they are not detected on biotin-coated beads (lanes 2 and 4). In order to quantify the interaction of MCa with RyR2, pull-down experiments were done with purified RyR2 in the presence of [^{3}H] ryanodine. The amount of RyR2-MCa complex was then assessed by measuring the [^{3}H] ryanodine bound onto the MCa coated beads. Results presented on Figure 1B shows the amount of [^{3}H] ryanodine labelled RyR2 pulled down as a function of MCa beads concentrations. The maximum binding value (Bmax) corresponds to the amount of [^{3}H] ryanodine bound to RyR2, measured under the same conditions by classical filtration approach. In the presence of 500 nM MCa, approximately 90% of the RyR is bound to MCa. These results highlight the presence of two populations of RyR within our preparation. The first one represents approximately 10% of the pulled down RyR and shows an apparent affinity for MCa of 10 nM similar to the apparent affinity previously measured for the MCa-RyR1 interaction. The second population represents the large majority of the pulled down RyR2 population and shows an apparent affinity for MCa of 150 nM. Although these two populations could represent two different state of the RyR2, they could also lead from a slight contamination of the preparation with RyR1. In this case one has to consider that since MCa induces an 8 to 10 folds increase of [^{3}H] ryanodine binding on RyR1, this contamination would, in fact, represents only 1% of the total RyR2 population. In both cases, these results show that MCa interacts with RyR2 although with an apparent affinity lower than with RyR1.

To further characterize the RyR2 domains interacting with MCa, we aligned the sequences of previously identified RyR1 MCa binding domains (namely the F3 and F7 domains [13]), with equivalent RyR2 sequences, using the CLUSTALW software [17] (http://www.ebi.ac.uk/clustalw). This comparison shows that fragments F3 and F7 share 54.2% and 63.2% amino acid identity with the corresponding fragments of RyR2. Based on this alignment, RyR2-F3 and F7 domains encompassing amino acids 1033-1622 and 3158-3609, respectively, were cloned and expressed *in vitro* as [^{35}S]-radiolabelled proteins. The

interaction of these fragments with MCa was then measured by pull-down experiments as described above. The results presented on figure 2A show that, similarly to RyR1-F3 and F7 domains, F3 and F7 domains of RyR2 specifically interact with MCa. Quantitative analysis (figure 2B) shows that ~15% of RyR2-F3 and ~50% of RyR2-F7 fragments are bound to MCa-coated beads.

Effect of MCa on [^{3}H]-ryanodine binding on RyR2.

As previously described, MCa is one of the most powerful effectors of RyR1 [7]. This effect of MCa has been associated to its interaction with discrete domains of RyR1 and deletion of the F7 domain leads to a RyR1 channel that is insensitive to MCa [13]. Since MCa interacts with homologous F3 and F7 fragments of RyR2, we evaluated the ability of MCa to modify RyR2 properties. We first studied the effect of MCa on [^{3}H]-ryanodine binding on SR vesicles enriched in RyR2, isolated from canine heart. The results presented on figure 3 show that, while MCa induces a strong increase of [^{3}H]ryanodine binding on RyR1 (8-folds increase of B_{max}, EC_{50} 10 nM), it promotes a very small and non saturating (up to 2 µM) effect on [^{3}H]-ryanodine binding on RyR2. Since RyR2 differs from RyR1 in its dependence to cytoplasmic Ca^{2+} concentration, the effect of MCa on RyR2 was also tested in the presence of higher calcium concentration (pCa 4). No significant changes were observed for the effect of MCa on RyR2 (data not shown).

Single channel analysis of MCa effects on RyR2 channel.

We next studied the effect of MCa on the gating properties of RyR2. Purified RyR2 was incorporated into an artificial lipid bilayer and MCa was added to the *cis* chamber which corresponds to the cytoplasmic face of the RyR2 channel. We previously showed that MCa affects the RyR1 gating behavior by inducing i) an increase of the opening probability (Po) and ii) the appearance of characteristic long lasting subconductance states (LLSS) [7]. These LLSS correspond to the opening RyR1 at an intermediate conductance state for extremely long periods of time, up to a few seconds.

Figure 4 shows representative traces of single RyR2 channel activity before and after application of 500 nM MCa onto the cytoplasmic side of RyR2 (*cis* chamber). Current recordings were performed by imposing two ionic current directions, corresponding to i) the "physiological direction", from the RyR2 luminal side (*trans* chamber) to the cytoplasmic side or ii) the "reverse direction", from the RyR2 cytoplasmic side to the luminal side. The results presented on figure 4 and table 1 evidence major differences in the effect of MCa on

RyR2 compared to its effect on RyR1: i) in the “physiological direction” of the ionic current, neither LLSS events nor significant change of Po were observed after addition of MCa on RyR2 (figure 3A); ii) in the “reversed direction” of the ionic current, addition of MCa induced the appearance of LLSS events on RyR2 (figure 3B) different from those observed on RyR1. Indeed, a statistical comparison of RyR1 and RyR2 LLSS induced by MCa in the “reverse direction” (table 1) shows a much shorter duration of RyR2 single LLSS (192.7 ±14.7 ms for RyR2 *vs* 12037 ± 875 ms for RyR1). In the “reverse direction” current condition, no significant change of Po value (measured during inter-LLSS periods) was observed in the presence of MCa.

MCa fails to induce Ca^{2+} release from cardiac SR vesicles.

In order to further investigate a possible effect of MCa on RyR2, we studied the ability of MCa to induce Ca^{2+} release from SR vesicles purified from canine heart. Cardiac SR vesicles were actively loaded with Ca^{2+} in the presence of pyrophosphate and then submitted to increasing concentrations of MCa. Extra-vesicular Ca^{2+} concentration changes were measured using Antipyrylazo III as calcium indicator. Figure 5 shows representative traces obtained with skeletal and cardiac SR vesicles. While MCa at 25 nM (final concentration) induces a strong and rapid Ca^{2+} release from skeletal SR vesicles it does not induce any Ca^{2+} release from cardiac SR vesicles even at 1 µM (final concentration). In order to assess the functional integrity of the cardiac SR vesicles and Ca^{2+} release process through RyR2, Ca^{2+} release was induced in presence of thymol, a previously described agonist of RyR2 [18]. As seen on figure 5B, addition of thymol (1.5 mM) induces Ca^{2+} release from cardiac SR vesicles demonstrating both the tight sealing of these vesicles and the functionality of RyR2. These results demonstrate that MCa is unable to induce Ca^{2+} release from cardiac SR vesicles.

Discussion

In the present study, we evaluated the putative activation of RyR2 by MCa. We demonstrate that MCa is able to interact directly with purified RyR2. This interaction involves at least two domains homologous to those of RyR1 previously identified as MCa binding sites. We also show that MCa does not induce any changes neither in [^{3}H]-ryanodine binding on RyR2 nor in RyR2 channel gating properties. In coherence with these results, we show that MCa fails to promote Ca^{2+} release from cardiac sarcoplasmic reticulum.

In previous works, we characterized MCa as one of the most powerful effectors of RyR1 [7] and identified two discrete domains (F3 and F7) of RyR1 responsible for the binding of MCa [13]. Here we show that despite the fact that MCa interacts with RyR2 on the domains homologous to F3 and F7, MCa is unable to induce the characteristic functional modifications that it promotes on RyR1. These results suggest that, while F3 and F7 domains are directly involved in the control of RyR1 gating process, they exert a completely different control on RyR2 gating behavior. Therefore, MCa presents specificity for the skeletal versus the cardiac RyR isoform in terms of functional effect while it does not show specificity in terms of interaction. MCa is to our knowledge the first molecule shown to interact with the homologous sequences of RyR1 and RyR2 and yet presents a completely different effect on each isoform. Imperatoxin A ($IpTx_a$) has been shown to modify, although to a much slighter degree than MCa, the gatting properties of RyR1 [19-21] and various degrees of effect of this toxin on RyR2 have been described [22, 23]. Therefore, in comparison with MCa, $IpTx_a$ shows a much weaker effect and a much less function specificity between RyR1 and RyR2.

A significant effect of MCa on RyR2 conductance was observed when the imposed current was in the opposite direction compared to the physiological situation during calcium release (positive potential). The subconductance events induced by MCa in these conditions were however much shorter than those observed on RyR1 at both positive and negative potentials. In its primary amino acid sequence, MCa presents a cluster of basic residues. Structural data show that these residues form a positively charged surface [6]. Consequently, at positive potential, the electric field could provoke an accumulation of MCa at the vicinity of the pore region of RyR2 responsible for the “conductance reducer” effect observed.

The effects of MCa on RyR1 indicate that MCa strongly activates RyR1 channel opening. This effect could result i) from the direct implication of the MCa binding sites (i.e.

F3 and F7 domains) in the pore forming region of RyR1 or ii) from the destabilization, following MCa binding, of an intra-molecular “brake” that would, through a distance effect, allow RyR1 opening. In the first hypothesis, the absence of MCa effect on RyR2 would suggest a complete different 3D topology of RyR2 channel moiety, excluding the homologous domains of F3 and F7 from the pore region. In the second hypothesis, the lack of MCa effect on RyR2 would highlight the presence on RyR2 of a different intra-molecular “brake” insensitive to MCa binding. Previous studies using chimeric RyRs have shown that the functional importance of a specific domain of RyR1 differs when this domain is expressed in a RyR3 or RyR2 background, revealing that several domains of RyRs are involved in the channel gating process [24, 25]. All together these results seem to favour the second hypothesis, the difference in MCa effect on RyR1 and RyR2 being due to the lack in RyR2 of signal transduction from the MCa binding domains to the pore domain.

Interestingly, we recently demonstrated that MCa shares common binding sites on RyR1 with a domain of the cytoplasmic II-III loop of the dihydropyridine receptor (DHPR) $Ca_v1.1$ subunit [13]. Based on the effect of MCa on calcium sparks in skeletal muscle cells and on the closure kinetics of RyR1 following the re-polarization of the plasma membrane, we proposed that this domain of the DHPR could be a regulator of the RyR1 internal “brake” [10, 11]. Therefore the absence of effect of MCa on RyR2 could reflect a physiological difference in the role of the corresponding domain of the cardiac DHPR $Ca_v1.2$ subunit in the control of RyR2 gating behavior.

Figure legends

Figure 1: MCa interacts with RyR2.

A, *Western blot analysis of pull-down experiments showing direct interaction of MCa with purified RyR1 and RyR2*. Purified RyR1 and RyR2 were obtained as described in Materials and Methods. Streptavidine-coated magnetic beads covered with either biotin or biotinylated MCa (MCa_b) were incubated with purified RyR1 or RyR2 and the bound proteins analysed as described under "Materials and Methods". **B**, *Concentration dependence relationship of the MCa-RyR2 interaction.* Purified RyR2 was incubated with increasing concentration of biot-MCa coated on streptavidin beads in the presence of 10 nM [^{3}H]-ryanodine for 90 min. at room temperature. Beads were then washed and [^{3}H]-ryanodine bound on MCa-beads measured by liquid scintillation. Unspecific binding was measured in the presence of 20 µM unlabeled ryanodine. The total amount of [^{3}H]-ryanodine-RyR complex (Bmax) was measured in identical conditions by filtration technique.

Figure 2: MCa interacts with discrete domains (F3 and F7) of RyR1 and RyR2.

A, RyR1 F3 and F7 domains and the corresponding domains of RyR2 were expressed *in vitro* as radiolabeled proteins (input lanes), as described in "*Experimental"*. Each fragment was then incubated in the presence of polystyrene magnetic beads coated either with biotin or biotinylated MCa (MCa_b). Interaction of each fragment with MCa-coated beads was measured by autoradiography after separation on SDS-PAGE. **B,** Statistical analysis of the interaction of *in vitro* translated F3 and F7 fragments of RyR with biotin (white boxes) or MCa_b (grey boxes for RyR1 fragments and black boxes for RyR2 fragments). Binding was estimated by densitometric analysis and expressed as the mean ± S.E.M. from at least three independent experiments.

Figure3: MCa does not modify [^{3}H]-ryanodine binding on RyR2.

[^{3}H]-ryanodine binding on skeletal and cardiac was measured in presence of 5 nM [^{3}H]-ryanodine and various concentrations of MCa as described in Materials and Methods. Multiplication factor of [^{3}H]-ryanodine binding on skeletal vesicles (opened symbols) and cardiac vesicles (closed symbols) are presented as a function of MCa concentration.

Nonspecific binding remained constant independently of MCa concentrations and represented less than 8% of total binding. Each point was done in triplicate.

Figure 4 : MCa effect on RyR2 gating properties.

Representative current traces of control and MCa-induced RyR2 channel activity. Purified RyR2 was incorporated in planar lipid bilayer and its single channel activity recorded as described under "*Experimental*". The holding potential was –80 mV in **A** and +80 mV in **B**. The conductance of RyR2 was approximately 500 pS. The time duration of each record is 20 s. The closed and opened states of the channel are designated by *C* and *O* respectively. MCa was applied at a concentration of 500 nM in the *cis* chamber containing a free Ca^{2+} concentration of 472 nM.

Figure 5: MCa fails to induce Ca^{2+} release from cardiac SR vesicles.

Representative traces of extra vesicular Ca^{2+} concentration variations measured using Antipyrylazo III Ca^{2+} indicator (see "*Experimental*"). Skeletal HSR vesicles (**A**) and cardiac HSR vesicles (**B**) were actively loaded with Ca^{2+} by sequential addition of 20 µM $CaCl_2$ in the cuvette. After Ca^{2+} addition, the absorbance was monitored until the initial baseline value was reached. MCa-induced Ca^{2+} release was tested on skeletal and cardiac HSR vesicles by addition of 25 nM MCa (skeletal HSR, **A**) and 1 µM MCa (cardiac HSR, **B**). Integrity of the cardiac vesicles and functionality of the RyR2 channel were assessed by injection of 1.5 mM thymol, 10 min after the application of MCa.

References

1 Fill, M. and Copello, J. A. (2002) Physiol Rev **82**, 893-922

2 Tanabe, T., Mikami, A., Numa, S. and Beam, K. G. (1990) Nature **344**, 451-3

3 Nakai, J., Ogura, T., Protasi, F., Franzini-Armstrong, C., Allen, P. D. and Beam, K. G. (1997) Proc Natl Acad Sci U S A **94**, 1019-22

4 el-Hayek, R., Lokuta, A. J., Arevalo, C. and Valdivia, H. H. (1995) J Biol Chem **270**, 28696-704

5 Zhu, X., Zamudio, F. Z., Olbinski, B. A., Possani, L. D. and Valdivia, H. H. (2004) J Biol Chem

6 Mosbah, A., Kharrat, R., Fajloun, Z., Renisio, J. G., Blanc, E., Sabatier, J. M., El Ayeb, M. and Darbon, H. (2000) Proteins **40**, 436-42

7 Esteve, E., Smida-Rezgui, S., Sarkozi, S., Szegedi, C., Regaya, I., Chen, L., Altafaj, X., Rochat, H., Allen, P., Pessah, I. N., Marty, I., Sabatier, J. M., Jona, I., De Waard, M. and Ronjat, M. (2003) J Biol Chem **278**, 37822-31

8 Tanabe, T., Beam, K. G., Adams, B. A., Niidome, T. and Numa, S. (1990) Nature **346**, 567-9

9 Dulhunty, A. F., Curtis, S. M., Watson, S., Cengia, L. and Casarotto, M. G. (2004) J Biol Chem **279**, 11853-62

10 Pouvreau, S., Csernoch, L., Allard, B., Sabatier, J. M., De Waard, M., Ronjat, M. and Jacquemond, V. (2006) Biophys J **91**, 2206-15

11 Szappanos, H., Smida-Rezgui, S., Cseri, J., Simut, C., Sabatier, J. M., De Waard, M., Kovacs, L., Csernoch, L. and Ronjat, M. (2005) J Physiol **565**, 843-53

12 Shtifman, A., Ward, C. W., Wang, J., Valdivia, H. H. and Schneider, M. F. (2000) Biophys J **79**, 814-27

13 Altafaj, X., Cheng, W., Esteve, E., Urbani, J., Grunwald, D., Sabatier, J. M., Coronado, R., De Waard, M. and Ronjat, M. (2005) J Biol Chem **280**, 4013-6

14 Marty, I., Robert, M., Villaz, M., De Jongh, K., Lai, Y., Catterall, W. A. and Ronjat, M. (1994) Proc Natl Acad Sci U S A **91**, 2270-4

15 Anderson, K., Lai, F. A., Liu, Q. Y., Rousseau, E., Erickson, H. P. and Meissner, G. (1989) J Biol Chem **264**, 1329-35

16 Lai, F. A., Erickson, H. P., Rousseau, E., Liu, Q. Y. and Meissner, G. (1988) Nature **331**, 315-9

17 Thompson, J. D., Higgins, D. G. and Gibson, T. J. (1994) Nucleic Acids Res **22**, 4673-80

18 Szentandrassy, N., Szigeti, G., Szegedi, C., Sarkozi, S., Magyar, J., Banyasz, T., Csernoch, L., Kovacs, L., Nanasi, P. P. and Jona, I. (2004) Life Sci **74**, 909-21

19 Valdivia, H. H., Kirby, M. S., Lederer, W. J. and Coronado, R. (1992) Proc Natl Acad Sci U S A **89**, 12185-9

20 Gurrola, G. B., Arevalo, C., Sreekumar, R., Lokuta, A. J., Walker, J. W. and Valdivia, H. H. (1999) J Biol Chem **274**, 7879-86

21 Zamudio, F. Z., Gurrola, G. B., Arevalo, C., Sreekumar, R., Walker, J. W., Valdivia, H. H. and Possani, L. D. (1997) FEBS Lett **405**, 385-9

22 Tripathy, A., Resch, W., Xu, L., Valdivia, H. H. and Meissner, G. (1998) J Gen Physiol **111**, 679-90

23 Simeoni, I., Rossi, D., Zhu, X., Garcia, J., Valdivia, H. H. and Sorrentino, V. (2001) FEBS Lett **508**, 5-10

24 Nakai, J., Sekiguchi, N., Rando, T. A., Allen, P. D. and Beam, K. G. (1998) J Biol Chem **273**, 13403-6
25 Perez, C. F., Voss, A., Pessah, I. N. and Allen, P. D. (2003) Biophys J **84**, 2655-63

FOOTNOTES

This work was supported by grants from the European Commission (HPRN-CT-2002-00331), Association Française contre les Myopathies, Hungarian research Found (OTKA T 61442) and by INSERM, CEA and UJF.

Table 1

Characterisation of the MCa effect on RyR2 gating behaviour.

Single channel recording of purified RyR2 or RyR1 incorporated in artificial lipid bilayer were performed as described under "*Experimental*". Physiological current direction corresponds to ionic flux from the luminal face of the RyR to its cytoplasmic face, while reverse current direction corresponds to an ionic flux from the cytoplasm face of the RyR to its luminal side.

	[MCa]	RYR2 Physiological current direction	RYR2 Reverse current direction	RYR1 Reverse current direction
Po				
	0	0.034 ± 0.014	0.007 ± 0.005	0.02 ± 0.007
	50 nM	0.061 ± 0.021	0.009 ± 0.003	0.21 ± 0.016
	100 nM	0.058 ± 0.020	0.011 ± 0.007	0.24 ± 0.021
	500 nM	0.068 ± 0.023	0.010 ± 0.008	0.31 ± 0.047
LLSS				
Number of events /min	0	0	0	0
	50 nM	0	136.3 ± 53.2	19.7 ± 9.3
Average duration (ms)	0	n.d.	n.d.	n.d.
	50 nM	n.d.	192.7 ± 14.7	12037 ± 875
	100 nM	n.d.	186.2 ± 33.5	10236 ± 187
	500 nM	n.d.	217.7 ±67.2	13371 ± 245

n.d.=non detectable

Figure 1

A

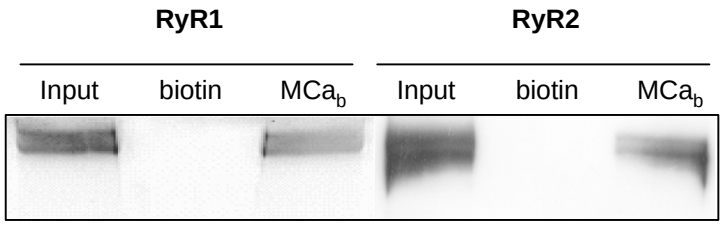
RyR1
RyR2
Input
biotin
MCa$_b$
Input
biotin
MCa$_b$

B

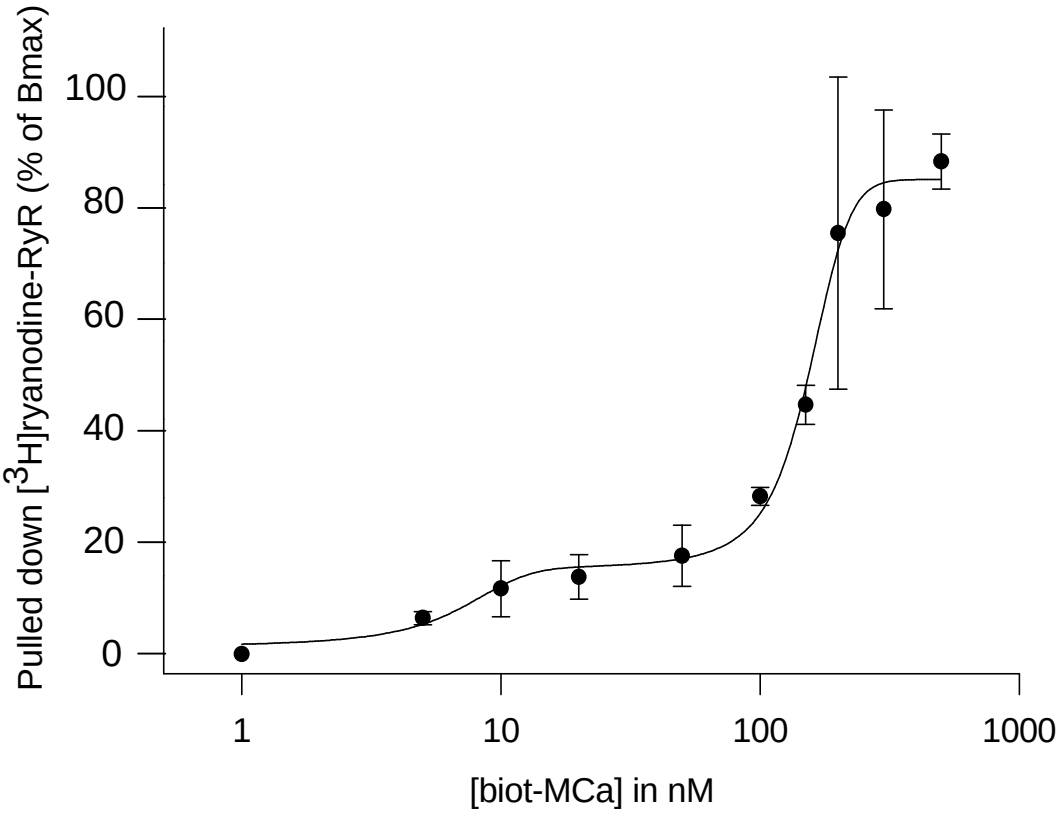
Pulled down [^{3}H]ryanodine-RyR (% of Bmax)
100
80
60
40
20
0
1
10
100
1000
[biot-MCa] in nM

Figure 2

A

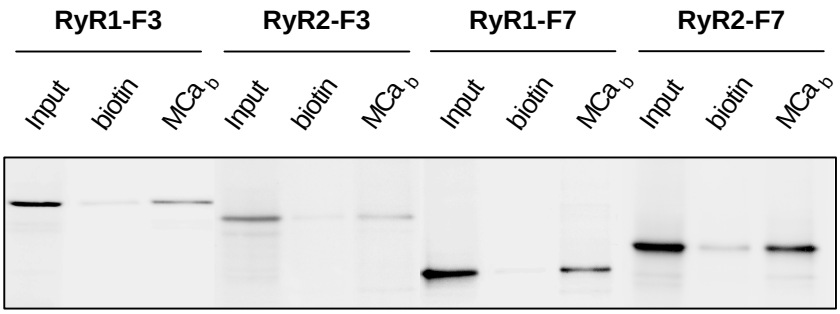
RyR1-F3
RyR2-F3
RyR1-F7
RyR2-F7
Input
biotin
MCa$_b$
Input
biotin
MCa$_b$
Input
biotin
MCa$_b$
Input
biotin
MCa$_b$

B

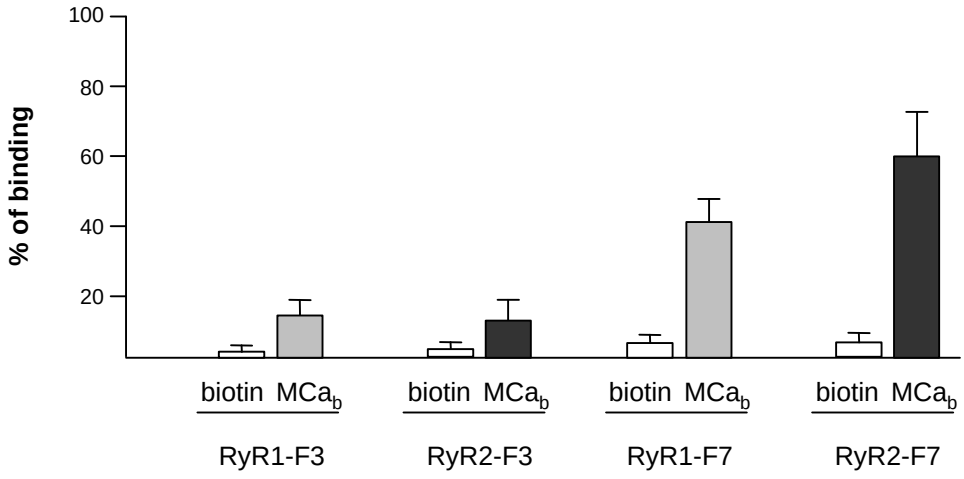
% of binding
100
80
60
40
20
biotin MCa$_b$
biotin MCa$_b$
biotin MCa$_b$
biotin MCa$_b$
RyR1-F3
RyR2-F3
RyR1-F7
RyR2-F7

Figure 3

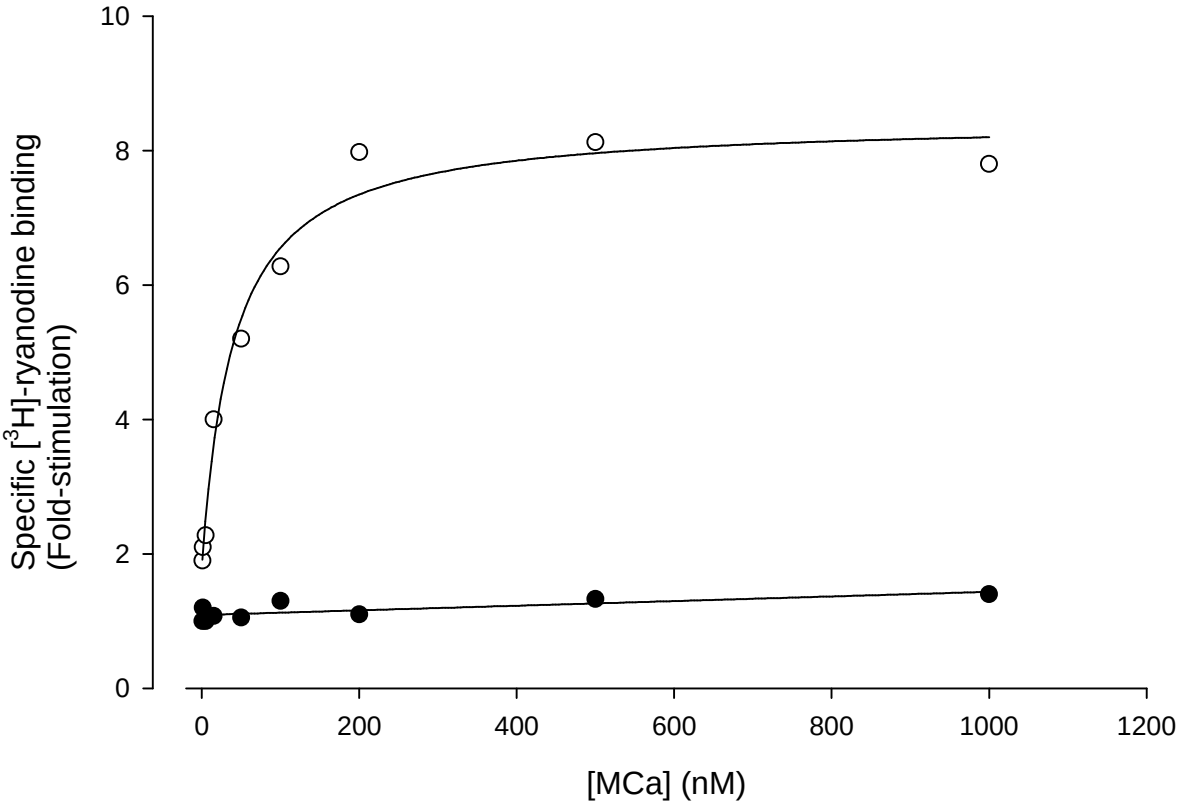
Specific [3H]-ryanodine binding
(Fold-stimulation)
10
8
6
4
2
0
0
200
400
600
800
1000
1200
[MCa] (nM)

Figure 4

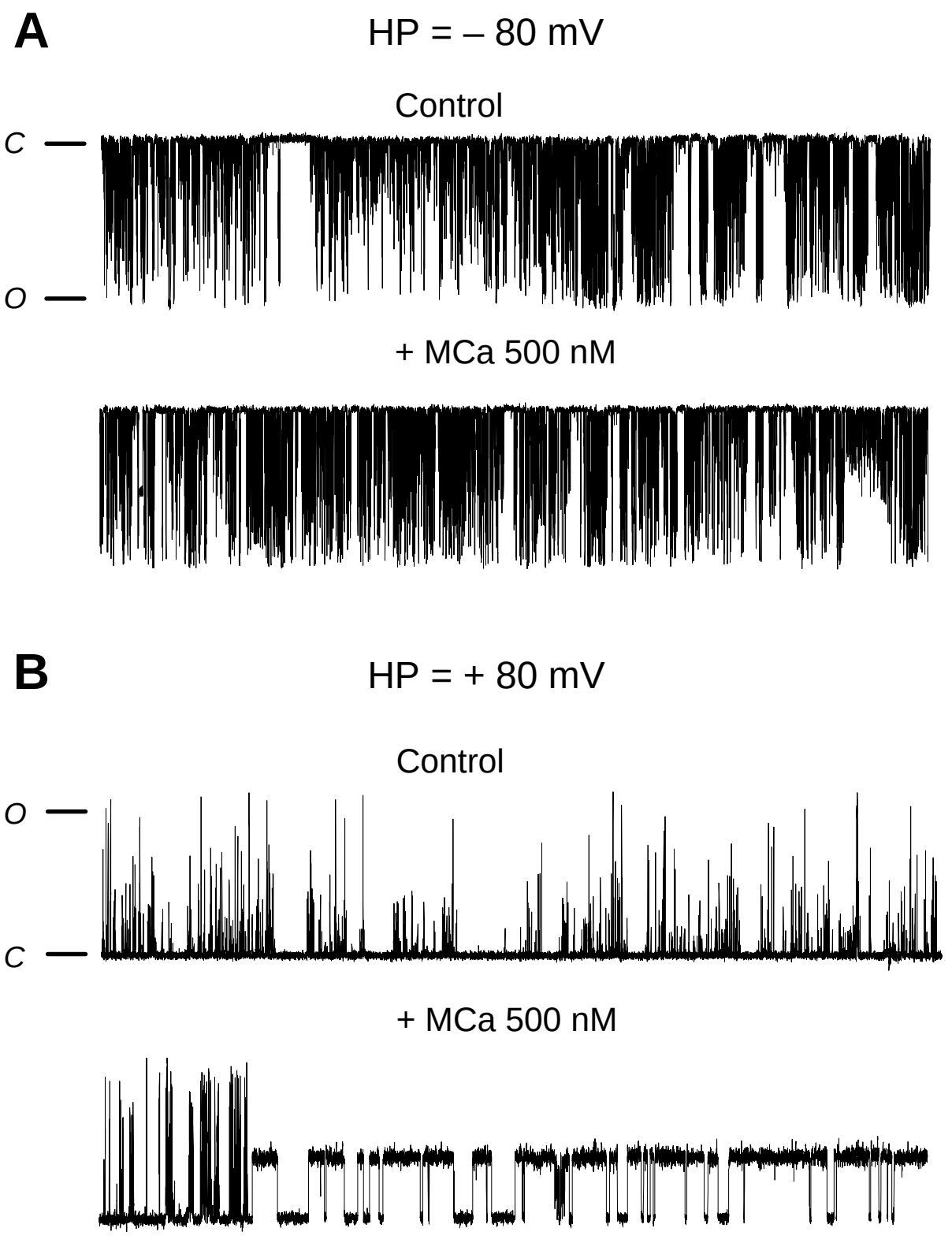

Figure 5

A

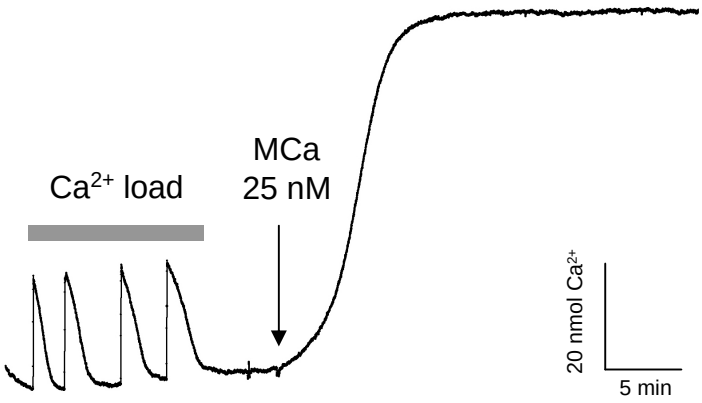
Ca2+ load
MCa
25 nM
20 nmol Ca2+
5 min

B

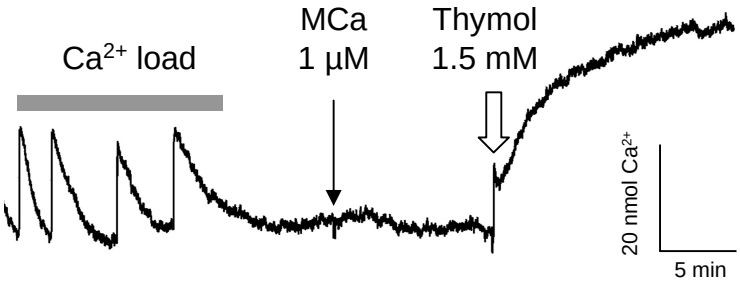
Ca2+ load
MCa
1 µM
Thymol
1.5 mM
20 nmol Ca2+
5 min